Reprogramming hormone-sensitive prostate cancer to a lethal neuroendocrine cancer lineage by mitochondrial pyruvate carrier (MPC)

Huan Xu [1,8], Zhixiao Liu [2,7,8], Dajun Gao [1,8], Peizhang Li [1], Yanting Shen [1], Yi Sun [3], Lingfan Xu [4], Nan Song [5], Yue Wang [2,****], Ming Zhan [1,***], Xu Gao [6,**], Zhong Wang [1,*]

ABSTRACT

Cell lineage reprogramming is the main approach for cancer cells to acquire drug resistance and escape targeted therapy. The use of potent targeted therapies in cancers has led to the development of highly aggressive carcinoma, including neuroendocrine prostate cancer (NEPC). Although metabolic reprogramming has been reported to be essential for tumor growth and energy production, the relationship between metabolic reprogramming and lineage differentiation which can cause hormone therapy resistance has never been reported in prostate cancer (PCa). Moreover, as there is still no efficient therapy for NEPC, it is urgent to reverse this lineage differentiation during the hormone therapy. Here for the first time, we used *in vitro* and *in vivo* human PCa models to study the effect of metabolic reprogramming on the lineage differentiation from the androgen receptor (AR)−dependent adenocarcinoma to AR-independent NEPC. This lineage differentiation leads to antiandrogen drug resistance and tumor development. This phenotype is enabled by the loss of mitochondrial pyruvate carrier (MPC), the gate for mitochondrial pyruvate influx, and can be reversed by MPC overexpression. Morphologic and cellular studies also demonstrate that the pyruvate kinase M2 (PKM2) involved epithelium−mesenchymal transition process mediated this lineage alteration. Its inhibition is a potential treatment for MPC-lo tumors. All of these results suggest that metabolic rewiring can act as a starter for increased cellular plasticity which leads to antiandrogen therapy resistance through lineage differentiation. This study provides us with a potent treatment target for therapy-induced, enzalutamide-resistant NE-like prostate cancer.

1. INTRODUCTION

Metabolic reprogramming is a significant hallmark of cancer [1]. Activation of oncogenes or loss of tumor suppressor genes, such as mutations in *PTEN, AKT, MYC,* and *TP53*, alters the cancer metabolic process [2]. The metabolic pathway itself also participates in the epigenetic regulation of gene expression, which is essential for embryonic development, differentiation, and cancer progression [3]. Thus, metabolic reprogramming is controlled by cancer-related genes and, in turn, modulates gene expression and activity in cancer development.

Pyruvate, as the main source of cellular acetyl-CoA, which is the most important cellular epigenetic factor, has been extensively studied in recent years [3−5]. Its metabolic process, especially pyruvate mitochondrial influx controlled by mitochondrial pyruvate carrier (MPC), contributes to stem cell maintenance and cancer initiation [6,7]. However, the effect and mechanism of metabolic rewiring on cancer lineage plasticity and drug resistance are still largely unknown.

Lineage plasticity contributes to the development and therapy resistance of solid cancers. PCa, having the highest estimated cancer incidence rate in males [8], presents sensitivity to hormonal therapy

[1]Department of Urology, Shanghai Ninth People's Hospital, Shanghai, China [2]Shanghai Key Lab of Cell Engineering, Shanghai, China [3]Guangdong Key Laboratory of Urology, Guangzhou, China [4]The First Affiliated Hospital of Anhui Medical University, Anhui, China [5]Department of Urology, Beijing Shijitan Hospital, Beijing, China [6]Department of Urology, Shanghai Changhai Hospital, Shanghai, China [7]Research Center of Developmental Biology, Department of Histology and Embryology, College of Basic Medicine, Naval Medical University, Shanghai, China

[8] These authors contributed equally to this article.

****Corresponding author. Shanghai Key Lab of Cell Engineering, 800 Xiangyin Road, Shanghai, 200433, China. E-mail: wangyuesmmu@163.com (Y. Wang).

*Corresponding author. Department of Urology, Shanghai Ninth People's Hospital, 639 Zhizaoju Road, Shanghai, 200011, China, Fax: +86 21 63136856. E-mail: zhongwang2000@sina.com (Z. Wang).

***Corresponding author. Department of Urology, Shanghai Ninth People's Hospital, 639 Zhizaoju Road, Shanghai, 200011, China, Fax: +86 21 63136856. E-mail: zhanming@shsmu.edu.cn (M. Zhan).

**Corresponding author. Department of Urology, Shanghai Changhai Hospital, 168 Changhai Road, Shanghai, 200433, China. Fax: +86 21 35030006. E-mail: gaoxu.changhai@foxmail.com (X. Gao).

targeting the androgen receptor (AR). Although the initial response is usually efficient, the development of castration-resistant PCa (CRPC) is nearly inevitable. The second-generation hormonal therapy drugs enzalutamide (MDV3100) and abiraterone acetate have proven to be effective against CRPC, but resistance persists. PCa shows a notable lineage differentiation after hormonal therapy and acquires therapeutic resistance by converting from adenocarcinoma to neuroendocrine prostate cancer (NEPC), also known as therapy-induced NEPC (t-NEPC). NEPC is composed entirely of NE cells and does not respond to hormonal therapy, including enzalutamide or abiraterone. Most primary PCa is histologically identified as adenocarcinoma, which is mainly composed of luminal-type cells. Less than 1% of primary PCa is considered to be caused by NEPC; however, the incidence of NEPC has increased to 30% in CRPC cases and is significantly associated with poor clinical outcomes [9]. Additionally, immunohistochemistry (IHC) staining of tissue has been the only method to detect and study NE cells [10]. The lack of a specific marker contributes to the poor diagnosis and prediction of NE tumor cells. The development of an AR-independent therapeutic strategy and a novel detection method for NEPC is urgently needed.

In this study, we investigated the role of MPC in PCa hormone therapy resistance and NEPC differentiation. We found that the decreased mitochondrial pyruvate influx induced by MPC inhibition converted prostate cancer cells from hormone-sensitive adenocarcinoma to NE-like cells, which are enzalutamide resistant. This study enriches our knowledge of metabolic reprogramming effects on PCa development and provides a novel candidate for the treatment and metabolic diagnosis of hormone therapy-resistant NE-differentiated PCa.

2. RESULTS

2.1. MPC is expressed at a low level in human NEPC cells
To determine the metabolic changes in PCa cells with NEPC characteristics, we performed metabolic profiling using LC/MS analyses with LNCaP-AR and LNCaP-AR-P53/RB-KO cell lines. The tricarboxylic acid cycle (TCA) level was decreased in the LNCaP-AR-P53/RB-KO cells, which are PCa cells with NEPC characteristics, compared with LNCaP-AR cells, which are CRPC adenocarcinoma cells [11], while the glycolysis rate was elevated (lactate, $p < 0.05$, Figure 1A). Pyruvate is the bridge between the TCA cycle and glycolysis. We speculated the decreased pyruvate mitochondria influx played important role in this metabolic switch. Neuron-specific enolase (NSE), an enolase 2 (ENO2) gene, is the most widely used NE marker. To find the most significant gene in which downregulation is correlated with both NEPC and the decreased pyruvate mitochondria influx, we analyzed all genes related to pyruvate mitochondria influx and NSE. MPC2 and MPC1 are most significantly positively correlated with the NSE RNA level among them (shown in Figure 1B, the dataset is shown in the Materials and Method section). Moreover, we selected the genes which are decreased in both basal cells and NEPC cells (compared with adenocarcinoma cells, the data are from Jiaoti Huang's Lab). Among them, MPC1 is the most significantly changed one (fold <0.5 both in basal cells and NEPC cells compared with adenocarcinoma cells, Figure 1C). MPC is the gate in the mitochondrial inner membrane enabling pyruvate mitochondrial influx, which is the bridge between glycolysis and the TCA cycle. MPC is a complex constituting two units (MPC1 and MPC2), and the loss of either unit makes the other unit unstable, decreasing its level. According to the dataset obtained from Beltran's study [12], MPC2 is expressed at low levels in human NEPC tissues (a p-value of MPC2 <0.05), though MPC1 is not decreased. RNA-Seq data obtained from Mu's study [11] showed that MPC2 expression was also decreased in

the LNCaP-AR-P53/RB-KO cell line compared with that in the LNCaP-AR cell line. Moreover, patient-derived PCa cells exhibited low expression of MPC1 and MPC2 in CXCR2+ NE cells (188.7 ± 23.9 FPKM) and basal cells (178.2 ± 10.9 FPKM) compared with CXCR2− luminal cells (377.8 ± 121.1 FPKM; the dataset was obtained from Jiaoti Huang's Laboratory [10]). All of the aforementioned data are shown in Figure 1D, E and Supplemental Fig. 1A. The CCLE (Broad Institute Cancer Cell Line Encyclopedia) data showed that in NPEC cell lines (NCIH660 and PC3 cells), both MPC1 and MPC2 were expressed at a lower level than in PCa adenocarcinoma cell lines. Although MPC1 was not expressed at low levels in NCI-HC660 cells, the MPC2 level was expressed at low levels (Figure 1F). Moreover, our evaluation of the TMAs (tissue microarrays) confirmed these results; MPC1 and MPC2 were present at low levels in NEPC cells compared with their levels in adenocarcinoma cells (Figure 1G). A gene set enrichment analysis (GSEA) based on RNA-Seq data [13] obtained from 65 patients with primary PCa indicated that the MPC1 level was negatively correlated with basal cell carcinoma and that the MPC2 level was negatively correlated with small cell cancer, indicating a negative correlation of the expression levels of both with an NE cell carcinoma signaling pathway (Figure 1H and Supplemental Fig. 1D). These findings support the notion that MPC-negative cells are enriched in NEPC tissue.

2.2. MPC is decreased after hormone therapy in prostate adenocarcinoma
Prolonged hormonal therapy may lead to NEPC, known as therapy-induced NEPC (t-NEPC), which shows enzalutamide resistance in clinical experiments. This study evaluated RNA-Seq data obtained from patients whose MPC levels were downregulated after Androgen deprivation therapy (ADT) treatment (Figure 1I and J). During cell culture, enzalutamide (added at two different doses, E1 at 10 μM and E2 at 20 μM) significantly reduced MPC2 expression. MPC1 expression was also significantly decreased in the 20 μM enzalutamide-treated cells. AR, as a transcription factor (TF), binds to the sequence AAG-GAGAGGGTGGGC in the promoter zone of MPC2 to induce transcription (Figure 1I). These findings demonstrate that MPC is downregulated after hormonal therapy and expressed at a low level in NEPC cells.

2.3. MPC downregulation promotes neuroendocrine differentiation (NED) in prostate adenocarcinoma
MPC is reduced in NEPC tissues and can be downregulated by hormone therapy. Metabolic reprogramming has been reported to be both a result of gene regulation and an influencer of cancer fate. These outcomes led us to further investigate the MPC effect on NED. After knocking out (KO) MPC2 and overexpressing (OE) MPC1 and MPC2 in the C4—2B cell line, we performed RNA-Seq and analyzed the small cell neuroendocrine cancer (SCNC)-specific accessible peaks [14], as shown in Figure 2A; and disease enrichment, as shown in Figure 2B (the details are shown in supplemental tables). Low MPC expression was enriched in neuroendocrine cells during differentiation, implicating basal cell-related pathways. Consistently, MPC2 KO and MPC overexpression elevated and suppressed the levels of NEPC markers, respectively (Figure 2C, D, and E), as indicated by protein levels in C4—2B, C4—2B enzalutamide-resistant (C4—2B MDVR) cells, 22RV1 cells, LNCaP-AR-P53/RB-KO cells, and PC3 cells. MPC2 KO facilitated NED progression of the adenocarcinoma cell lines (22RV1, C4—2B, and C4—2B MDVR cells), while MPC overexpression suppressed SYP expression in the PC3 cells. As double knockdown of TP53 and RB1 has been reported to be critical for NEPC differentiation, we also evaluated the LNCaP-AR-P53/RB-KO cell line [11], which is NEPC-like
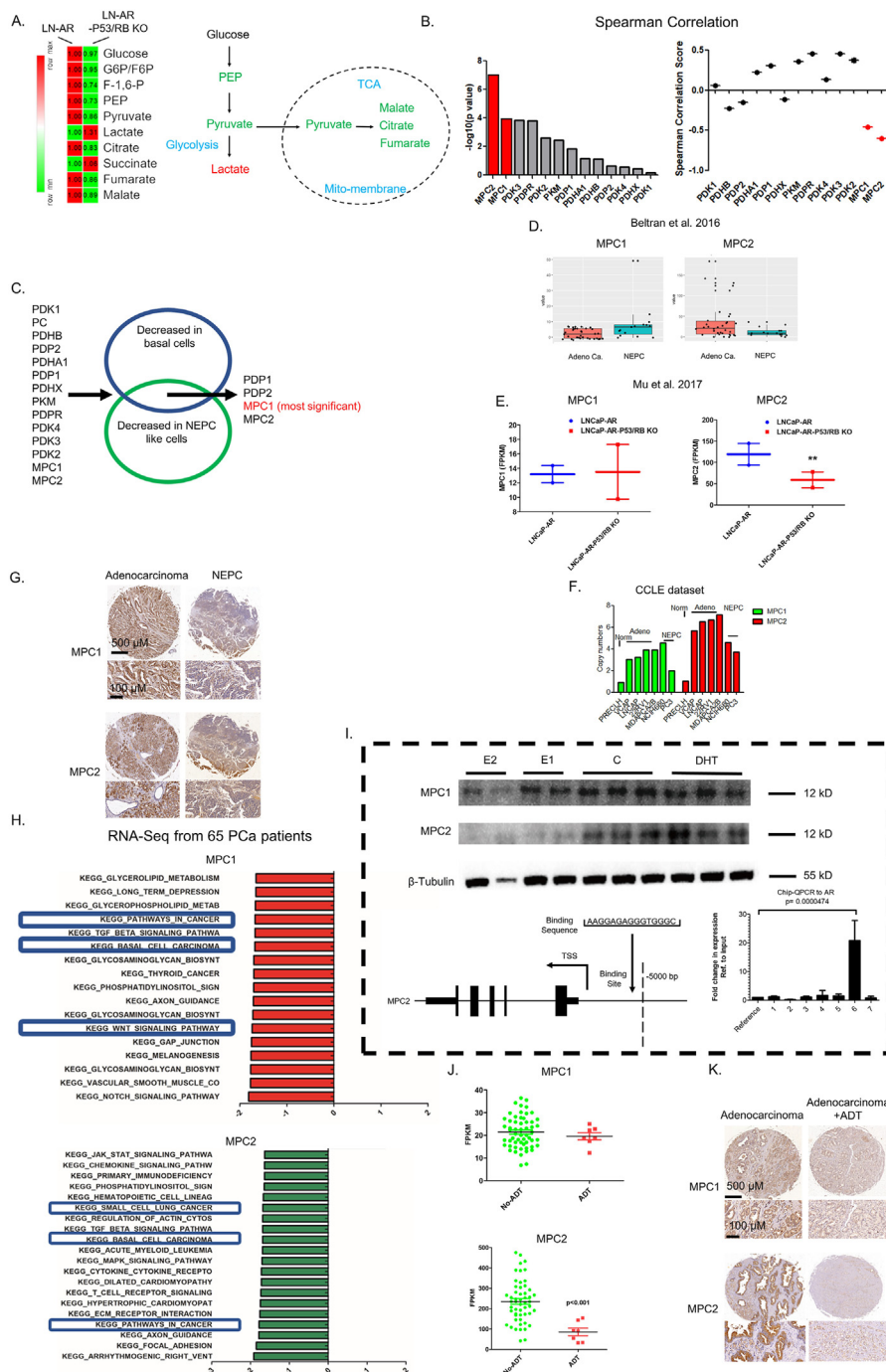
Figure 1: MPC is expressed at a low level in NEPC cells. A. Metabolic profiling of the CRPC adenocarcinoma cell line (LNCaP-AR cells) and CRPC NEPC cell line (LNCaP-AR-P53/RB-KO cells). Red: level increased, green: level decreased, black: level unchanged. B. Spearman correlation analysis between genes related to mitochondria pyruvate influx and NSE (NEPC marker). Data are from tissues of 65 prostate cancer patients. MPC1 and MPC2 are most significantly correlated with NSE levels. C. MPC is the most significant gene change both in basal cells and PCa cells with NEPC characteristics compared with adenocarcinoma cells. Genes which are related to pyruvate mitochondria influx are listed left. Genes which are both decreased in basal cells and NEPC like cells are selected and MPC1 is the most significantly changed one. These data are from Jiaoti Huang's Lab. D. Analysis of MPC expression in adenocarcinoma and NEPC cells. The adenocarcinoma and NEPC datasets were obtained from Beltran's laboratory (RNA-Seq data were derived from patient tissue). E. Analysis of MPC expression of LNCaP-AR and LNCaP-AR-P53/RB-KO data which were obtained from Mu Ping's study. F. MPC1 and MPC2 expression in different cell lines according to the CCLE dataset. G. Representative images of MPC IHC staining of TMAs (above, overall view; below, 20 × view). Four NEPC patient tissues and 184 adenocarcinoma patient tissues were included in the array. H. GSEA of MPC1 and MPC2, which was found to be expressed at low levels in patient tissues on the basis of RNA-Seq data obtained from 65 primary patients [13]. I. MPC level changes in patient PCa tissues after ADT. Data are from PCa patient RNA-Seq data [13]. J. MPC levels after enzalutamide (E1, 10 μM; E2, 20 μM) and DHT (dihydrotestosterone) treatment. ChIP-QPCR data of the AR binding point to the MPC2 promoter sequence. K. MPC level changes of patient TMAs after the ADT procedure (100 × view). Unless otherwise noted, in each panel, the mean ± SEM (error bars) is represented. P values were calculated using t-tests. N.S., not significant. *P < 0.05, **P < 0.01.
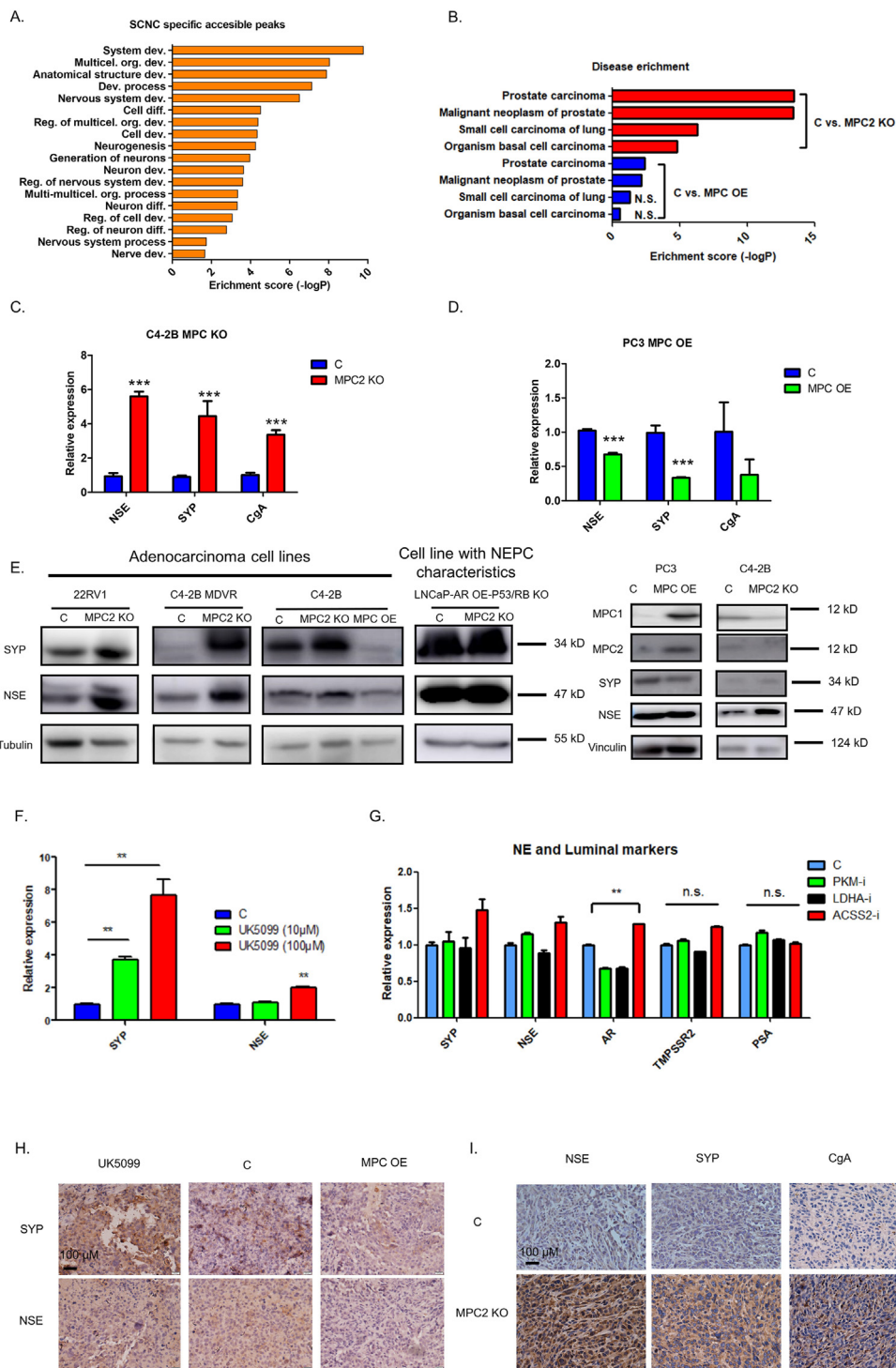
Figure 2: Downregulation of MPC promotes NE differentiation. A. Gene Ontology terms for small cell neuroendocrine carcinoma (SCNC)-specific accessible peaks of the MPC2-KO C4—2B cell line. B. Disease enrichment analysis of the MPC2-KO and MPC-OE C4—2B cell lines (*compared with the 10 μM groups; #compared with the 100 μM groups). C. The changes in the mRNA levels of NE markers in C4—2B MPC2-KO cells. D. The changes in the mRNA levels of NE markers in PC3 MPC-OE cells. E. The changes in the protein levels of NE markers in MPC2-KO cells and MPC-OE cells. In the C4—2B cell line (left part), MPC2 was first knocked out and then overexpressed (MPC-OE cells) in a rescue experiment. F. The changes in mRNA levels of NE markers after UK5099 (MPC inhibitor, 10 μM and 100 μM) treatment. G. The changes in mRNA levels of NE markers after different inhibitor treatments. PKM-i, 50 μM; ACSS2-i, 20 μM; and LDHA-i, 10 μM. H. IHC staining of NE markers (NSE and SYP) in PC3, PC3 UK5099 (6 mg/kg BW)-treated and PC3-MPC-OE xenograft mouse tumors. I. IHC staining of NE markers (NSE, SYP, and CgA) in LNCaP-control and LNCaP-MPC2-KO xenograft mouse tumors. Unless otherwise noted, in each panel, the mean ± SEM (error bars) are represented. P values are calculated using t tests. N.S., not significant. *$P < 0.05$, **$P < 0.01$, ***$P < 0.001$.
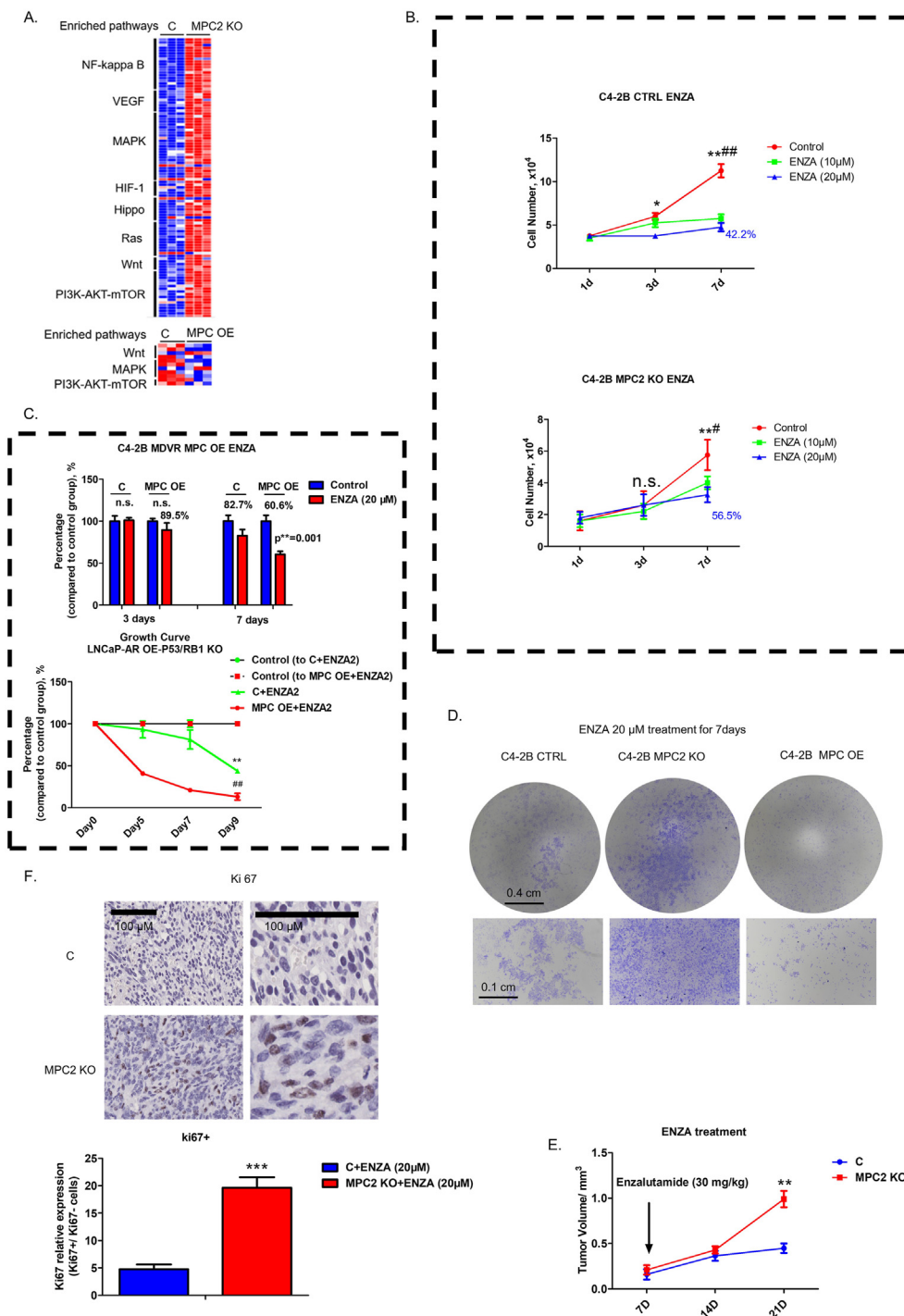
Figure 3: MPC regulates enzalutamide sensitivity. A. Heat map of enzalutamide resistance-related pathways in C4—2B MPC2-KO cells. B. Enzalutamide resistance changes in C4—2B and C4—2B MPC2-KO cell lines. C. Enzalutamide resistance changes in MPC-OE cell lines, namely, C4—2B MDVR (enzalutamide/MDV3100 resistant) and LNCaP-AR-P53/RB KO cell lines. D. Effect of 7-day enzalutamide treatment on the number of MPC2-KO/MPC-OE cells. E. Enzalutamide treatment on tumor sizes in a mouse xenograft model. The bar presents 1 cm. F. Ki67 staining in LNCaP-empty vehicle control (C) and LNCaP-MPC2-KO (MPC2 KO) tumors removed from xenograft mouse models treated with enzalutamide (30 mg/kg body weight, n = 4). Unless otherwise noted, in each panel, the mean ± SEM (error bars) is represented. The P values were calculated using t tests. N.S., not significant. *P < 0.05, **P < 0.01, ***P < 0.001.

and enzalutamide less sensitive, and found that MPC downregulation did not elevate NEPC marker levels. In C4—2B cells, MPC was over-expressed after being initially knocked out in a rescue experiment, and NE markers were also decreased significantly after overexpression (C4—2B cells in Figure 2E). Furthermore, we used the MPC inhibitor UK5099 at two doses to observe the blockade of NED by MPC (shown in Figure 2F,G, and Supplemental Fig. 2D). To observe the effect of the pyruvate pathway on NED, different key enzyme inhibitors (PKM-i,
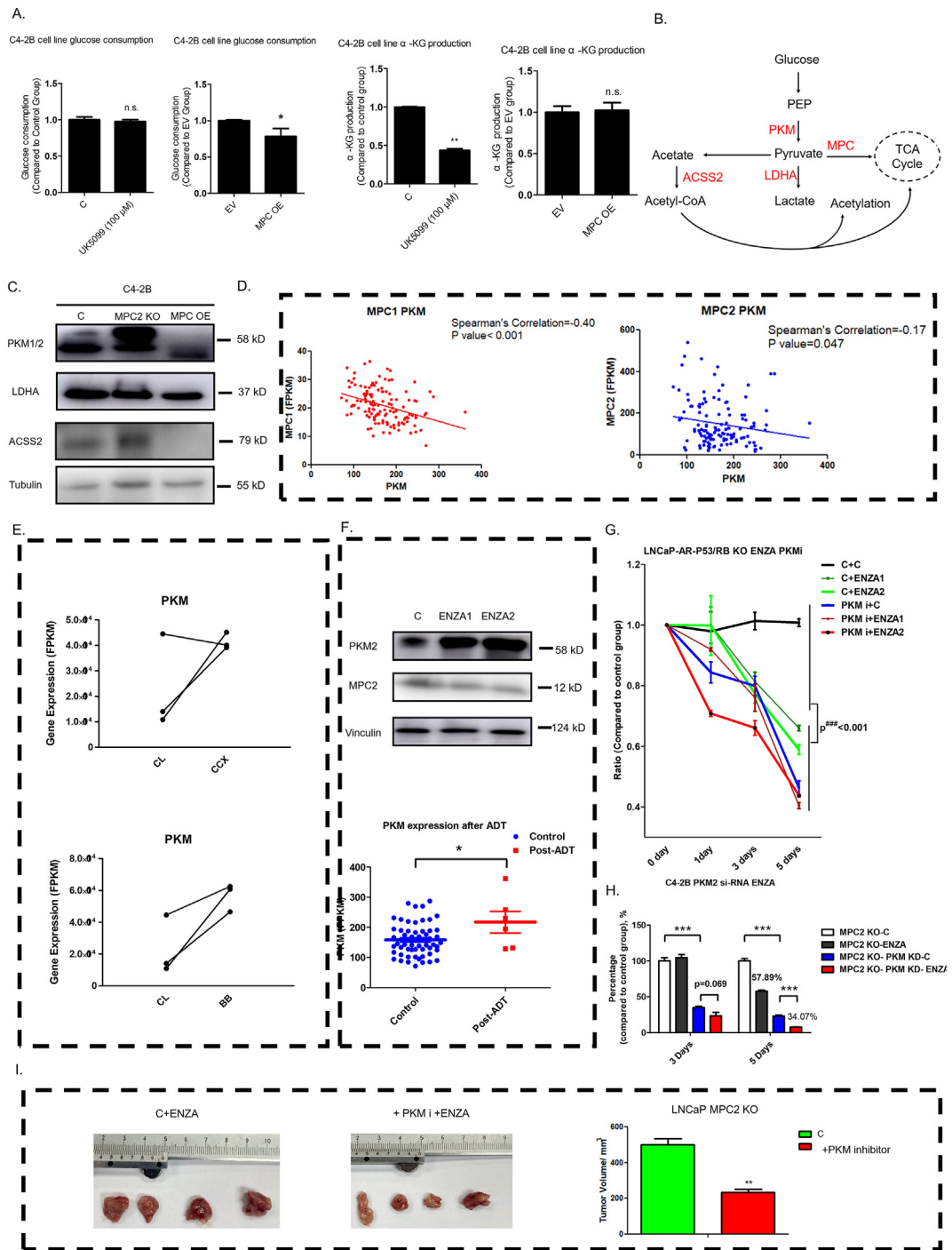
Figure 4: The block of PKM inhibits the growth of MPC lowly expressed PCa cells. A. Glucose consumption and α-KG change after MPC is blocked or overexpressed. B. Schematic figure of pyruvate metabolism pathways. C. Protein levels of key enzymes in pyruvate metabolism pathways after MPC2 KO or MPC overexpression. D.The correlation between MPC and PKM expression as determined with RNA-Seq data of PCa patients [13]. E. PKM RNA level in NEPC cells in different datasets. The data were obtained from datasets of patient-derived CXCR2+ NE (CCX) cells, CXCR2⁻ luminal cells (CL), and basal body (BB) cells.F. Enzalutamide effect on PKM2 expression at the protein level in C4−2B cells and the ADT effect on PKM RNA levels in the PCa patient RNA-Seq dataset. G. Effect of a PKM inhibitor (50 μM) on enzalutamide sensitivity of LNCaP-AR-P53/RB-KO cells. H. PKM KD effect on the enzalutamide sensitivity of C4−2B cells. I. PKM inhibitor decreases the growth of LNCaP-MPC2 KO tumors. Unless otherwise noted, in each panel, the mean ± SEM (error bars) is represented. The P values were calculated using t tests. N.S., not significant. *P < 0.05, **P < 0.01, ***P < 0.001.

LDHA-i, and ACSS2-I at the doses presented in the Figure legends) were used in a subsequent study and were not found to promote the NED process, in contrast to the effect of UK5099 (Figure 2F,G).

Moreover, subcutaneous PC3-MPC-OE tumors presented low expression of SYP and NSE compared with the control group, and 2 weeks of UK5099 treatment (6 mg/kg body weight) tended to elevate

NE marker expression (Figure 2H). NE marker expression was significantly increased in LNCaP-MPC2-KO tumors compared to LNCaP tumors in the xenograft mouse models (figure 2I). All of the aforementioned results demonstrate that the overexpression of MPC decreases NED, while MPC downregulation accelerates the NED process in adenocarcinoma PCa.

2.4. Low MPC expression elevates enzalutamide resistance in prostate adenocarcinoma

NEPC cells are not sensitive to enzalutamide, a next-generation anti-androgen drug, which renders these cells difficult to treat in clinical studies. The analysis of the RNA-Seq data suggested that MPC2-KO cells were highly enriched in hormone resistance-related cell signaling pathways (as determined by KEGG analysis, Figure 3A and supplemental materials). In this study, we did not observe a proliferation-promoting effect of MPC2 KO in studies performed in vivo or in vitro (Supplemental Figs. 3A and B). Intriguingly, MPC2 KO augmented enzalutamide resistance in the adenocarcinoma and NEPC cell lines with high AR expression (shown in Figure 3B,D). MPC overexpression increased enzalutamide sensitivity in different cell lines (shown in Figure 3C,D). This effect was also evident in the LNCaP-AR-P53/RB-KO cell line, indicating that the increased enzalutamide sensitivity was independent of P53 and RB regulation. LNCaP and LNCaP-MPC2-KO xenograft mouse models were assessed to confirm these results. After 2 weeks of enzalutamide treatment (intraperitoneal injection of 30 mg/kg body weight), the tumor volume of the LNCaP-MPC2-KO mice was significantly larger than that of the control mice with the empty vehicle control cells (Figure 3E, 0.99 ± 0.09 vs. 0.45 ± 0.05 mm^3, $p < 0.01$). Ki67-positive expression was also significantly higher in the MPC2-KO tumors than in the control tumors (19.68 ± 1.9 vs. 4.8 ± 0.9, $p < 0.001$).

2.5. PKM mediates MPC-induced enzalutamide resistance

To investigate the changes in glucose uptake after MPC activity was blocked, we added 100 μM UK5099 to treat cells. As shown in the MS analysis of the C4—2B cells (Figure 4A), although α-KG production was significantly downregulated after inhibitor treatment, glucose consumption was not changed significantly. This result might imply that glucose and pyruvate are catabolized in some salvage pathways. The three main pathways for pyruvate catabolism are shown in Figure 4B. We detected the key enzymes of each pathway and found that PKM and ACSS2 protein levels were significantly elevated, while no significant changes in lactate dehydrogenase (LDHA) levels were observed (Figure 4C). PKM mRNA levels were significantly and negatively correlated with MPC1 and MPC2 levels in the primary PCa RNA-Seq dataset [13] (Figure 4D; MPC1, $p < 0.001$; MPC2, $p = 0.047$). In the datasets obtained from the CCLE and those describing Jiaoti Huang's patient-derived NE cells, PKM was upregulated in NEPC-like cells and tissues (Figure 4E) and was negatively correlated with MPC expression. After ADT treatment, PKM mRNA levels were significantly elevated in both the cell experiments and data in the primary PCa RNA-Seq dataset [13] ($p < 0.05$), while the MPC level was decreased (Figure 4F). We directed different inhibitors to the key enzymes in each pathway, which confirmed that PKM and ACSS2 inhibitors suppressed the growth of MPC2-KO cells the most significantly (Supplemental Fig. 4C). Moreover, PKM-i and si-PKM treatment elevated enzalutamide sensitivity in C4—2B and LNCaP-AR-P53/RB-KO cells (Figure 4G,H). In the xenograft mice model, PKM inhibitor injection decreases the LNCaP-MPC2 KO tumor growth significantly ($p < 0.001$, Figure 4I).

2.6. MPC2 KO promotes the EMT

During the cell culture procedure, we found that the cellular morphology was significantly altered in the MPC2-KO and MPC-OE cells compared with the control cells. The GSEA indicated that the EMT, one of the most important mechanisms for NED and hormone resistance, was significantly augmented in the C4—2B MPC2-KO cells but was significantly diminished in the C4—2B MPC-OE cells (Figure 5A,B, Supplemental Fig. 5A). We further found that MPC2-KO switched cells from the epithelial type to the mesenchyme-like type as indicated by morphological observations and elevated mesenchyme-related markers, while MPC overexpression had the opposite effects (Figure 5C—E). In Figures 5E and 6B and C, we extracted nuclei protein for nuclei protein level analysis. We used lamin B, which is the component of the nuclear lamina and mainly expressed in nuclei [15], for loading control. Vinculin is an actin-binding protein enriched at cellular matrix but not in nuclei [16]. It is used, in our study, to detect the efficiency of nuclei extraction. In xenograft mouse models, the levels of epithelial markers were decreased, while those of mesenchymal markers were elevated in the LNCaP-MPC2-KO cells compared with the control LNCaP cells (Figure 5F).

2.7. MPC regulates the EMT and NED through PKM2 nuclear expression

PKM2 nuclear expression plays important role in the EMT [4,17]. In this study, we observed that the nuclear translocation of PKM2 was upregulated after si-MPC2 treatment, as shown in Figure 6A. We extracted nuclear proteins from the cells and found that PKM2 and β-catenin expression was elevated significantly after 72 h of treatment with si-MPC2 (Figure 6B and Supplemental Fig. 5B). We confirmed this effect using an MPC overexpression plasmid to perform transient transfection and found that the PKM2 and TWIST1 levels were reduced 72 h after transfection of the overexpression plasmid and in stable MPC-OE cell lines (Figure 6C and Supplemental Fig. 5C). Acetyl-CoA is important for the dissolution of PKM2 and is primarily derived from glucose in cells [3]. Thus, we cultured the cells in a glucose-depleted medium and found that the upregulating effect of MPC2 KD on PKM2 was diminished (Figure 6D). Serum deprivation activated chaperone-mediated autophagy (CMA), which was involved in acetyl-CoA-induced PKM degradation (Figure 6F). In cells cultured in FBS-deprivation medium, MPC2 KD elevated PKM2 levels, which indicates that acetyl-CoA might have been involved in this effect (Figure 6E). The level of acetyl-CoA was decreased in the MPC2-KO cells and upregulated in the MPC-OE cells (Figure 6G). PKM siRNA was used to evaluate the effects of PKM on MPC-induced EMT. After PKM knockdown, the elevating effect of MPC2 on the expression of NE and EMT markers disappeared (Figure 6H). All these results indicate that MPC downregulated the EMT, possibly through acetyl-CoA-induced PKM2 nuclear expression.

3. DISCUSSION

NEPC cells are found in high numbers in CRPC, although they constitute no more than 1% of all tumor cells in primary human PCa. The hormone therapy currently used in the clinic mainly targets adenocarcinoma cells with positive AR expression. Specifically, CRPC adenocarcinoma tumors have previously been shown to undergo lineage switching or NEPC differentiation (NED) under selective pressures during AR inhibition and transform into NE tumors, which ultimately cause treatment-induced NEPC (t-NEPC) [18]. NEPC is an important cause of therapy failure and PCa progression. There is no effective treatment, and the details of
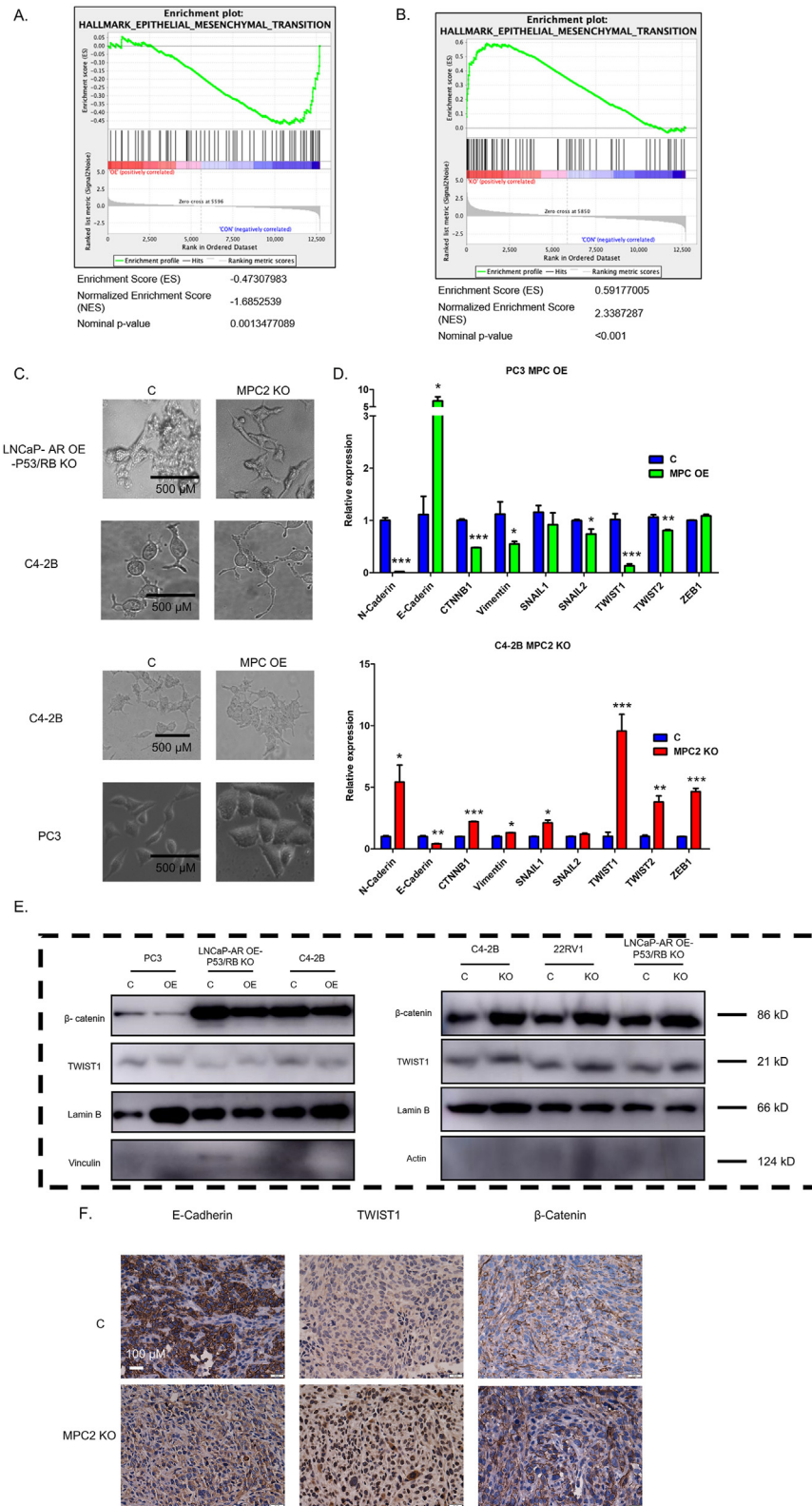
Figure 5: EMT participates in MPC-induced plasticity differentiation from adenocarcinoma into NE-like prostate cancer. A. Expression of EMT-related genes in C4—2B MPC-OE cells as determined by gene set enrichment analysis. B. Expression of EMT-related genes in C4—2B MPC2-KO cells as determined by gene set enrichment analysis. C. Representative images of MPC2-KO and MPC-OE cells with the EMT phenotype. D. RNA levels of EMT factors in C4—2B MPC2-KO and PC3 MPC-OE cells. E. Nuclear expression of β-catenin and TWIST1 in MPC2-KO and MPC-OE cell lines. KO: MPC2 KO; OE: MPC OE. F. IHC staining of E-cadherin, TWIST1 and β-catenin in LNCaP and LNCaP-MPC2-KO xenograft mouse models. Unless otherwise noted, in each panel, the mean ± SEM (error bars) is represented. P values were calculated using t tests. N.S., not significant. *P < 0.05, **P < 0.01, ***P < 0.001.
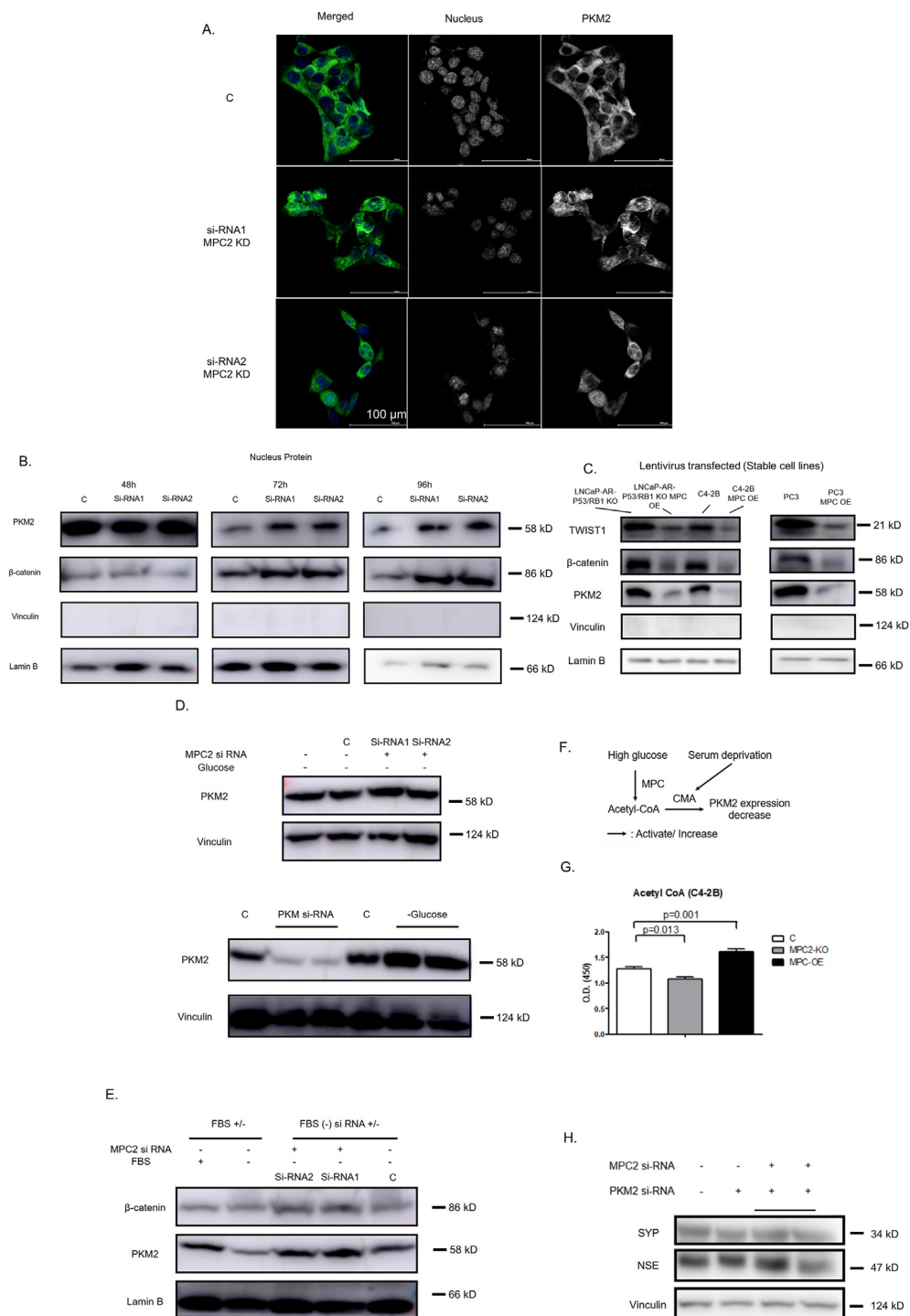
Figure 6: PKM2 nucleus expression mediates MPC-induced EMT in the NED process. A. Nuclear translocation of PKM2 in si-MPC2-treated C4—2B cells. B. Nuclear protein levels of PKM2 and β-catenin in MPC2-KD cells. C. Nuclear protein levels of PKM2, β-catenin, and TWIST1 in MPC-OE cells. D. PKM2 changes under different culture conditions (glucose deprivation) after treatment with si-MPC2. E. PKM2 changes in cell cultures with/without FBS after treatment with si-MPC2. F. Schematic figure of the acetyl-CoA-induced regulation of PKM2 expression. G. Acetyl-CoA level in MPC2-KO and MPC-OE C4—2B cells. H. Changes in NE marker levels in C4—2B-PKM2-KD cells treated with si-MPC2. No significant increase in NE markers exists in MPC2 KD cells after PKM2 being knocked down. Unless otherwise noted, in each panel, the mean ± SEM (error bars) is represented. The P values were calculated using t tests. N.S., not significant. *P < 0.05, **P < 0.01, ***P < 0.001.

this metabolic reprogramming have not been extensively studied yet. Metabolic reprogramming, as a critical hallmark of cancer, is not a mere consequence of cell fate; it is an influential factor of cancer cell fate. Mitochondrial pyruvate carrier (MPC) has been previously shown as a

gate in the mitochondrial inner membrane that enables pyruvate entry and further oxidation [19,20]. Recent studies have highlighted the impact of pyruvate oxidation on colon cancer initiation and stem cell maintenance [6]. However, the metabolic behavior of cell lineage

plasticity, which is significant for cancer development and treatment resistance, is almost completely unknown.

In this study, we demonstrate, for the first time, that MPC was significantly expressed at low levels in NEPC cells and that its downregulation contributed to NED and enzalutamide resistance. Moreover, MPC overexpression increased enzalutamide sensitivity and reversed NED in adenocarcinoma prostate cancer. These effects were likely mediated through the EMT induced by nuclear PKM2 translocation, which is controlled by acetyl-CoA, a product of pyruvate catabolism. PKM inhibitor can inhibit the growth of MPC lowly expressed cancers, as there is still no MPC agonist. These results indicate that metabolic rewiring can act as a starter for increased cellular plasticity which leads to antiandrogen therapy resistance through lineage differentiation.

In humans, MPC contains two distinct units, MPC1 and MPC2. The absence of either unit renders the other unstable, leading to reduced mitochondrial pyruvate uptake [21]. Thus, to induce MPC downregulation, only one MPC unit needs to be knocked out. However, to obtain an overexpressed stable cell line, both MPC1 and MPC2 need to be overexpressed [6,21]. According to the dataset and TMAs used in this study, MPC was significantly expressed at a low level in NEPC tissue and NEPC cell lines. Moreover, ADT decreased MPC levels both in patients in vitro (Figure 1I,J). In Figure 1I, only MPC2 is shown to be downregulated by enzalutamide treatment. CHIP-qRT-PCR results also confirmed that AR, the transcriptional factor, could bind to the promoter zone of MPC2 but not in MPC1. In another research, the researcher also reported that MPC2 was an AR-driven metabolic enzyme [22]. Either MPC1 or MPC2 is decreased, the MPC complex is unstable, and pyruvate mitochondria influx is downregulated [21]. To determine whether MPC downregulation is involved in the t-NEPC differentiation process, we knocked out MPC2 (MPC2 KO) in different adenocarcinoma and NEPC-like cell lines and confirmed the results with xenograft mouse models. MPC2 KO promoted NED in both hormone-sensitive PCa and CRPC adenocarcinoma (Figure 2C,D, E). Moreover, the MPC inhibitor UK5099 was also shown to accelerate NED, while other inhibitors of the pyruvate catabolism pathway did not exhibit similar effects (Figure 2F,G). As previously reported, pyruvate oxidation plays an important role in stem cell maintenance and cell fate decisions [7,23]. Pyruvate metabolism reprogramming, as a microenvironmental factor, might take part in the regulation of oncogene expression during cancer development. Multiple oncogenes contribute to NPEC development. The genomic landscape analysis of prostate cancer revealed that alterations in three genes, *AR, TP53,* and *RB1* are significantly altered in NEPC relative to primary prostate cancer, which effect is mediated by *SOX2* [11]. In another study, Jung Wook Park et al. reprogrammed normal human epithelial tissues to the lethal neuroendocrine cancer lineage by modulating the gene panel of five genetic factors, namely *TP53 (TP53DN), myrAKT1, RB1, c-Myc,* and *BCL2,* which are hereafter referred to as PARCB. Primary basal epithelial cells can be switched into NEPC cells by lentivirally transducing the PARCB factors, indicating that this gene panel plays important role in this lineage plasticity [14]. According to a large cohort of patients (37 NEPC, 169 PCA, 22 BEN), Himisha Beltran et al. demonstrated an increased expression of *AURKA* and *MYCN* in 40% of NEPC and 5% of PCA patients [24]. Although MPC2 loss could not completely switch the cell lineage from adenocarcinoma to NEPC in our study, it promoted the NED process and transformed cells into NE-like cells, leading to an increased frequency of NEPC lesion genesis. Thus, this study demonstrates that the mitochondrial pyruvate influx mediated by MPC regulates the NED process in PCa adenocarcinoma and reveals a metabolic basis for NEPC generation.

Hormone therapy resistance is a significant hallmark of NED that results in poor prognosis in the clinic. In this study, we evaluated changes in the sensitivity of cells and tumors to enzalutamide (MDV3100), a next-generation hormone therapy, and found that MPC downregulation elevated enzalutamide resistance in adenocarcinoma cell lines and xenograft mouse models. However, MPC overexpression did not elevate the enzalutamide sensitivity of 22RV1 cells, in which the drug resistance mechanism is related to AR splicing (ARV7). Although it has been previously reported that MPC downregulation accelerated cell proliferation, no significant changes in vitro or in vivo were observed in the present study (Supplemental Figs. 3A and B). Unexpectedly, this enzalutamide resistance-promoting effect of MPC2 KO was also observed in the LNCaP-AR-P53/RB-KO cell line, which has been reported to be an AR-overexpressing NEPC cell line, which showed a modest reduction in enzalutamide sensitivity [11]. These findings indicate that the effect of MPC on enzalutamide sensitivity might be dependent on the TP53 and RB1 regulation pathways. Thus, in previous clinical studies, potent AR inhibitors suppressed MPC expression, which led to NED and enzalutamide resistance.

In the bioinformatics analysis, the epithelial—mesenchymal transition (EMT) process was positively enriched (p < 0.001) in MPC2-KO C4—2B cells and negatively correlated (p < 0.05) with EMT-related genes in MPC-OE C4—2B cells (Figure 5A). During cell culture, the cellular morphology was observed to be significantly different after the MPC level was changed (Figure 5B). It has been established that NE tumor cells are enriched in gene sets associated with the EMT, and this gene set is similar to an enriched gene set activated in nonresponders to enzalutamide [25]. Many investigators have demonstrated that the change of a single EMT-inducing transcription factor (TF) is sufficient to induce a partial EMT program leading to the complete conversion of epithelial cells into mesenchymal cells [26]. These data indicate a close relationship between pyruvate metabolism and the EMT process. Pyruvate metabolism not only delivers energy for cell growth but also functions as a regulator of gene transcription [3]. In our study, although pyruvate influx into mitochondria was limited, glucose consumption was not decreased (Figure 4A). Glucose is mainly transformed into pyruvate in cellular plasma. There are three main mechanisms of pyruvate catabolism: pyruvate oxidation in mitochondria, lactate pathway functions, and acetate transformation outside of mitochondria. MPC2 KO and MPC overexpression significantly changed the expression of PKM and ACSS2, while no significant changes were observed in the LHDA level. Inhibitors of PKM and the three aforementioned catabolism pathways were analyzed to detect enzalutamide sensitivity and NED (Figure 2F,G and Supplemental Fig. 4C) and confirm that the pathway with MPC2 KO was elevated. These results indicate that the PKM2-related pathway might be a salvage pathway that is activated when mitochondrial pyruvate influx is blocked. As the key enzyme for pyruvate production, PKM consists of two different isotypes, PKM1 and PKM2. As is generally accepted, PKM1 mainly functions as an enzyme for pyruvate metabolism, while PKM2 was translocated to the nucleus as a transcriptional regulator (Figure 6A). It has been reported that the binding of PKM2 with TGIF2 recruits histone deacetylase 3 to the E-cadherin promoter sequence and regulates β-catenin (*CTNNB1*) transactivation, supporting the EMT process [4,17,27,28]. PKM2 degradation was also shown to be induced by acetyl-CoA through chaperone-mediated autophagy (CMA), which can be activated by serum deprivation. Therefore, we used PKM siRNA, glucose and serum deprivation to confirm the effect of PKM2 on the MPC-induced EMT. We observed that decreased MPC expression reduced acetyl-CoA levels, leading to elevated PKM2 expression, which led to the EMT and NED transformation. Moreover, the

translocation of PKM2 into the nucleus was augmented after MPC2 knockdown (MPC KD). After glucose depletion, which is the main trigger of acetyl-CoA production, MPC downregulation failed to influence the PKM2 protein level (Supplemental Fig. 4B and Figure 6B). In prostate cancer, PKM2 has been proved to play key roles in the castration or therapy resistance evolution, androgen receptor pathway reprogramming, and metabolic adaption to the nutritionally deprived and hypoxia conditions [29]. In neuroendocrine carcinoma cells, PKM1 is reported to be highly expressed in pulmonary neuroendocrine tumors, which is required for small cell lung cancer cell proliferation [30]. In *in-vivo* models, mice deficient in PKM2 specifically exhibit enhanced tumorigenesis in several experimental models [31,32]. Hence, MPC-PKM2-EMT might result in NED and enzalutamide resistance during hormone therapy. A search of Cancer Dependency Map (https://www.broadinstitute.org/cancer/cancer-dependency-map) revealed that PKM2 is not an essential gene indicating it might be a candidate for NEPC treatment in the future. This is the first study, to our knowledge, to demonstrate PKM2 regulation as a mechanism by which MPC regulates the EMT (Figure 7). As there is still no MPC agonist which can limit the PCa development, PKM inhibitor can be a good candidate for the treatment of MPC-lo cancers.

In this study, we used multiple model systems and methods, but there are still a few limitations. First, an MPC agonist has not been discovered to date. Although we observed that the overexpression of MPC reduced the NED process and enzalutamide resistance in adenocarcinoma prostate cancer, no currently available drug can be used as a treatment. Second, MPC could be a key metabolic regulator of NED; however, it cannot switch the lineage from normal epithelial cells into NEPC. Further genetic regulation studies are needed to determine the combined effect of different oncogenes with MPC on lineage switching. Third, despite the compelling data presented here, the real implications of our findings need to be tested in clinical settings to determine whether patients with advanced PCa benefit from MPC regulation.

In conclusion, MPC is expressed at a low level in NEPC tissue and plays an important role in the process of therapy-induced NEPC and hormone therapy resistance in PCa. The PKM-involved pathway is a salvage pathway in cells expressing low MPC levels and promotes the EMT process, which is a potential therapy for MPC-lo cancers. Accordingly, metabolic reprogramming should be treated more as a starter for the lineage plasticity and NEPC differentiation, instead of merely a result.

4. METHODS

4.1. Study design

The objective of this study was to investigate the effect of MPC and mitochondrial pyruvate influx on NEPC differentiation. Using RNA-seq datasets, metabolic profiling, and tumor microarray (TMA) data, we demonstrated that NE cells presented low MPC expression combined with limited mitochondrial pyruvate influx. MPC expression was also negatively correlated with small cell and basal cell carcinoma, according to a GSEA. As MPC expression is induced by AR and can be downregulated by hormone therapy, we hypothesized that decreased MPC levels during PCa development contribute to NED and enzalutamide resistance. Different PCa cell lines and xenograft mouse models were used to evaluate this hypothesis. During the experiment, the EMT was clearly observed, and EMT molecules were partially activated after MPC2 KO/KD. Different pyruvate catabolic pathways were studied, and PKM2, which is regulated by the MPC product acetyl-CoA, was
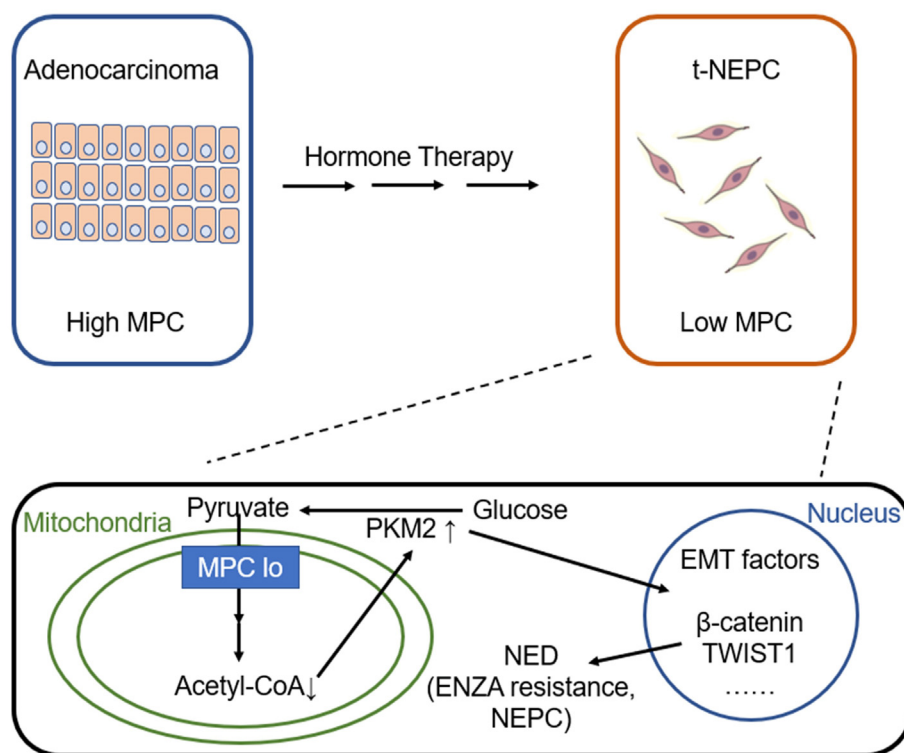

Figure 7: Schematic figure of MPC loss-induced NED and enzalutamide resistance. Prolonged hormone therapy reduces MPC expression and limits mitochondrial pyruvate influx. MPC downregulation contributes to the decrease in cellular acetyl-CoA level, which upregulates PKM2 nuclear translocation and expression. PKM2 nuclear levels promote EMT, which is critical for NE differentiation (NED) and hormone therapy resistance.

observed to function as an important modulator of the EMT and NED in MPC-low PCa cells.

4.2. PCa tissues and TMA samples

In the primary dataset of prostate cancer, 65 patients were involved with a range of prostate tumor grades and stages from treatment-naive Chinese patients for whole-genome and transcriptome sequencing. Treatment-naive PCa tumors were collected through radical prostatectomy from Shanghai Changhai Hospital and Fudan University Shanghai Cancer Center, China. Our data have already been published in 2017 [13].

Our TMA samples were obtained from the Department of Urology in Changhai Hospital, and ethical approval was obtained from the Medical Ethics Review Committee of Changhai Hospital. The number of prostate cancer patients was 210. The characteristics of patients are presented in supplemental figures and tables. The online tool used for calculating the sample size was http://powerandsamplesize.com/Calculators/TestTime-To-Event-Data/Cox-PH-2-Sided-Equality. TMA construction was performed as previously published [33]. The H-score was calculated as follows: percent of weak staining (scale: 0—100) *1 + percent of moderate staining (scale: 0—100)*2 + percent of strong staining (scale: 0—100)*3.

4.3. Public datasets

The RNA-seq dataset of CRPC adenocarcinoma and CRPC small-cell cancer in Beltran's study was evaluated [12]. RNA-Seq data of LNCaP-AR-P53/RB KO and LNCaP-AR cells from Mu's study were obtained [11]. The RNA-seq dataset from patient-derived CXCR2+ NEPC and basal cells from Jiaoti Huang's laboratory was obtained [10]. Expression data of different cancer cell lines were obtained from the public dataset Broad Institute Cancer Cell Line Encyclopedia (CCLE, https://portals.broadinstitute.org/ccle/about).

4.4. Immunohistochemical staining (IHC) and immunofluorescence (IF)

Tissue sections were incubated overnight with primary antibody at 4 °C after deparaffinization, rehydration in citrate buffer, and boiling in a water bath for 40 min, followed by incubation with horseradish peroxidase-conjugated goat anti-rabbit secondary antibody for 30—90 min at room temperature. Antibody binding was visualized using a 2-solution DAB kit (Invitrogen, 882,014). For the immunofluorescence analysis of cells, fluorescent secondary antibodies were added to cell cultures for 30—90 min. DAPI was used to identify nuclei. Images were obtained by laser-scanning confocal microscopy. IHC score from 0 to 3 was measured in this test.

4.5. Protein extraction and western blot analysis

Cell samples were stored at −80 °C until use, which were lysed in RIPA Lysis buffer with protease and phosphatase inhibitors. Protein concentration was determined with a Pierce BCA protein assay kit (Thermo Scientific). The loading buffer was loaded according to the instructions. Equal amounts of protein from samples were separated by 15% SDS-PAGE Gel and transferred to PVDF membrane (Millipore) using a semidry transfer system with 200 mA for 120 min. The antibodies used for Western blotting are shown in the supplemental materials.

4.6. RNA isolation and quantitative RT-PCR

Total RNA from cultured cells was extracted using TRIzol reagent (Invitrogen). Quantitative real-time PCR (qRT-PCR) assays were carried out to detect mRNA expression using the Prime Script RT Reagent Kit (RR037B, TaKaRa, USA) and SYBR green (RR820B, TaKaRa, USA) according to the manufacturer's instructions.

4.7. Cell lines

In this study, different cell lines, namely LNCaP, LNCaP-AR, LNCaP-AR-P53/RB-KO, PC3, C4—2B, C4—2B MDVR, and 22RV1 cells were used in experiments. To construct MPC-overexpressing cell lines, plasmid DNA of human MPC1 (NM_016,098 CDS) and human MPC2 (NM_015,415 CDS) were cloned into a pLenti-EF1a-EGFP-P2A-blasticidin-CMV-MCS vector. The plasmid pLenti-EF1a-EGFP-P2A-blasticidin-CMV-MPC1-P2A-MPC2 was used for lentivirus packaging using vectors pVSVG-I and pCMV-GAG-POL, which were obtained from Shanghai Integrated Biotech Solutions Co., Ltd. (Shanghai, China). To construct MPC2-KO cell lines, pLenti-U6-spgRNA v2.0-CMV-Blasticidin-P2A-3Flag-spCas9 was used as the vector and control treatment. After designing three target sequences, the sequence 'CCACTTTATCGAGGAGCCGG' was used for generating MPC2-KO cells. In this research, we knocked out or knocked down MPC2 to reduce the MPC complex level and the mitochondria pyruvate influx. For MPC2 RNA interruption, three different siRNAs were designed and their effects detected. For the PKM2 siRNA, we used a sequence described in a previous study [17]. The sequences are presented in the supplemental materials. Enzalutamide at 10 μM and 20 μM was added to the medium as a treatment during cell culture. Cells were treated with UK5099 (MCE, PF-1005023) in two doses (UK1 at 10 μM and UK2 at 100 μM), LHDA inhibitor was added at 10 μM, PKM-i was added at 50 μM, and an ACSS2 inhibitor was added at 20 μM.

The cell lines used in our research have their own characteristics and we designed the experiment according to this. LNCaP is a PCa adenocarcinoma cell line that is abundant with AR, sensitive to ADT and enzalutamide therapy. LNCaP-AR cell is LNCaP with AR overexpressed. It is resistant to ADT but sensitive to enzalutamide. LNCaP-AR-P53/RB KO is a PCa cell line with NEPC characteristics that is resistant to both ADT and enzalutamide. The C4-2 cell line is originated from the LNCaP cell line and resistant to ADT. However, the C4-2 cell line is sensitive to enzalutamide which is the next-generation hormone therapy in PCa. C4-2/MDVR cells were produced after 6-months of treatment with enzalutamide. It is an adenocarcinoma cell line but with enzalutamide resistance characteristics. The PC3 cell line is NEPC like cell line with AR loss and resistance to enzalutamide [34—36]. 22RV1 is an androgen-resistant cell line that expresses the AR and its splice variant 7 and the luminal epithelial markers. In summary, the characteristics of the above cell lines are as the followings: LNCaP (AR+/NE-), LNCaP AR OE-P53/RB KO (AR+/NE+), C4—2B (AR+/NE-), C4—2B MDVR (AR+/NE-), DU145 (AR-/NE-), PC3 (AR-/NE+). 'NE+' means NE markers positive.

4.8. Xenograft mice models

Nude (nu/nu) mice were purchased from Shanghai Laboratory Animal Center (SLAC, China). All of the procedures are approved by the Ethics Committee of Shanghai 9th People's Hospital (SH9H-2021-A122-SB). A total of 5×10^6 LNCaP transfected with empty vehicle or LNCaP-MPC2-KO cells were suspended in 0.1 ml of PBS and inoculated subcutaneously into six-week-old male nude mice. The tumor volume was calculated using the formula volume (mm^3) = (length × height2)/2. After the mice were euthanized with CO_2, xenografts tumors were harvested, fixed in 10% formalin, and embedded in paraffin for further analysis. Enzalutamide was administered twice a week through intraperitoneal injection at a dose of 30 mg/kg body mass for 2 weeks; 4—6 mice were used in this study.

4.9. Nuclei protein extraction

Cell samples were frozen at −80 °C until use. To obtain total protein, the cells were lysed in RIPA lysis buffer containing protease and phosphatase inhibitors following standard procedures. For nuclear proteins, a nucleoprotein extraction kit from Sangon Biotech (C500009, Shanghai, China) was used according to the manufacturer's protocol.

4.10. Metabolic profiling

Metabolites were extracted in 80% cold methanol followed by speed vacuum drying after the cells were harvested. The dried pellets were subjected to LC/MS analyses. The detailed procedures were reported in our previous publication [37].

4.11. ChIP

ChIP was performed using Simple ChIP Enzymatic Chromatin IP Kit (Magnetic Beads) (CST, #9003, USA). Approximately 2×10^7 cells were performed for each immunoprecipitation. Normal IgG served as a negative control. Precipitated DNA was analyzed by qRT PCR technique using the FastStart Universal SYBR Green Master. A standard curve was prepared for each set of primers using a serial titration of the input DNA. The percentage of ChIP DNA was calculated relative to the input DNA from primer-specific standard curves.

4.12. Statistical analysis

Bioinformatic analyses were performed using R Project for Statistical Computing, Statistica, and GraphPad. The information is indicated in the figure legends, results, materials and methods.

Statistics were performed using SPSS software (version 19.0; SPSS Inc., Chicago, IL, USA), and figures were generated with GraphPad Prism 5 (San Diego, CA, USA). Correlation analysis was used by Spearman's and Pearson's correlation analysis. A P-value of <0.05 was considered statistically significant.

Details on the patient characteristics, plasmid and siRNA sequences, RNA-Seq data of the MPC2-KO cells, and cell production information are available in the supplemental materials.

PROTOCOL

The protocol (including the research question, key design features, and analysis plan) was prepared before the study and this protocol was registered in the Review Committee of the 9th **disclosure statement** The authors declare no potential conflicts of interest.

CONSENT FOR PUBLICATION

Informed consent for publication was obtained from all participants.

DATA AVAILABILITY

All of the data included in this research are available if needed.

ETHICS APPROVAL AND CONSENT TO PARTICIPATE

This project was approved by the Clinical Research Ethics Committee of Shanghai ninth people's Hospital associated with Shanghai Jiaotong University.

FUNDING

ACKNOWLEDGMENTS

CONFLICT OF INTEREST

None declared.

APPENDIX A. SUPPLEMENTARY DATA

Supplementary data to this article can be found online at https://doi.org/10.1016/j.molmet.2022.101466.

REFERENCES

[1] DeBerardinis, R.J., Lum, J.J., Hatzivassiliou, G., Thompson, C.B., 2008. The biology of cancer: metabolic reprogramming fuels cell growth and proliferation. Cell Metabolism 7(1):11–20.

[2] Lv, L., Li, D., Zhao, D., Lin, R., Chu, Y., Zhang, H., et al., 2011. Acetylation targets the M2 isoform of pyruvate kinase for degradation through chaperone-mediated autophagy and promotes tumor growth. Molecular Cell 42(6):719–730.

[3] Sutendra, G., Kinnaird, A., Dromparis, P., Paulin, R., Stenson, T.H., Haromy, A., et al., 2014. A nuclear pyruvate dehydrogenase complex is important for the generation of acetyl-CoA and histone acetylation. Cell 158(1):84–97.

[4] Yang, W., Xia, Y., Ji, H., Zheng, Y., Liang, J., Huang, W., et al., 2011. Nuclear PKM2 regulates beta-catenin transactivation upon EGFR activation. Nature 480(7375):118–122.

[5] Ruiz-Iglesias, A., Manes, S., 2021. The importance of mitochondrial pyruvate carrier in cancer cell metabolism and tumorigenesis. Cancers (Basel) 13(7).

[6] Bensard, C.L., Wisidagama, D.R., Olson, K.A., Berg, J.A., Krah, N.M., Schell, J.C., et al., 2020. Regulation of tumor initiation by the mitochondrial pyruvate carrier. Cell Metabolism 31(2):284–300 e287.

[7] Wei, P., Dove, K.K., Bensard, C., Schell, J.C., Rutter, J., 2018. The force is strong with this one: metabolism (Over)powers stem cell fate. Trends in Cell Biology 28(7):551–559.

[8] Siegel, R.L., Miller, K.D., Fuchs, H.E., Jemal, A., 2021. Cancer statistics, 2021. CA: A Cancer Journal for Clinicians 71(1):7–33.

[9] Santoni, M., Conti, A., Burattini, L., Berardi, R., Scarpelli, M., Cheng, L., et al., 2014. Neuroendocrine differentiation in prostate cancer: novel morphological insights and future therapeutic perspectives. Biochimica et Biophysica Acta 1846(2):630–637.

[10] Li, Y., He, Y., Butler, W., Xu, L., Chang, Y., Lei, K., et al., 2019. Targeting cellular heterogeneity with CXCR2 blockade for the treatment of therapy-resistant prostate cancer. Science Translational Medicine 11(521).

[11] Mu, P., Zhang, Z., Benelli, M., Karthaus, W.R., Hoover, E., Chen, C.C., et al., 2017. SOX2 promotes lineage plasticity and antiandrogen resistance in TP53- and RB1-deficient prostate cancer. Science 355(6320):84–88.

Original Article

[12] Beltran, H., Prandi, D., Mosquera, J.M., Benelli, M., Puca, L., Cyrta, J., et al., 2016. Divergent clonal evolution of castration-resistant neuroendocrine prostate cancer. Natura Med 22(3):298—305.

13 Ren, S., Wei, G.H., Liu, D., Wang, L., Hou, Y., Zhu, S., et al., 2018. Whole-genome and transcriptome sequencing of prostate cancer identify new genetic alterations driving disease progression. European Urology 73(3):322—339.

[14] Park, J.W., Lee, J.K., Sheu, K.M., Wang, L., Balanis, N.G., Nguyen, K., et al., 2018. Reprogramming normal human epithelial tissues to a common, lethal neuroendocrine cancer lineage. Science 362(6410):91—95.

[15] Constantinescu, D., Gray, H.L., Sammak, P.J., Schatten, G.P., Csoka, A.B., 2006. Lamin A/C expression is a marker of mouse and human embryonic stem cell differentiation. Stem Cells 24(1):177—185.

[16] Bays, J.L., DeMali, K.A., 2017. Vinculin in cell-cell and cell-matrix adhesions. Cellular and Molecular Life Sciences 74(16):2999—3009.

[17] Hamabe, A., Konno, M., Tanuma, N., Shima, H., Tsunekuni, K., Kawamoto, K., et al., 2014. Role of pyruvate kinase M2 in transcriptional regulation leading to epithelial-mesenchymal transition. Proceedings of the National Academy of Sciences of the U S A 111(43):15526—15531.

[18] Chen, R., Dong, X., Gleave, M., 2018. Molecular model for neuroendocrine prostate cancer progression. BJU Int 122(4):560—570.

[19] Bricker, D.K., Taylor, E.B., Schell, J.C., Orsak, T., Boutron, A., Chen, Y.C., et al., 2012. A mitochondrial pyruvate carrier required for pyruvate uptake in yeast, Drosophila, and humans. Science 337(6090):96—100.

[20] Herzig, S., Raemy, E., Montessuit, S., Veuthey, J.L., Zamboni, N., Westermann, B., et al., 2012. Identification and functional expression of the mitochondrial pyruvate carrier. Science 337(6090):93—96.

[21] Schell, J.C., Olson, K.A., Jiang, L., Hawkins, A.J., Van Vranken, J.G., Xie, J., et al., 2014. A role for the mitochondrial pyruvate carrier as a repressor of the Warburg effect and colon cancer cell growth. Molecular Cell 56(3):400—413.

[22] Bader, D.A., Hartig, S.M., Putluri, V., Foley, C., Hamilton, M.P., Smith, E.A., et al., 2019. Mitochondrial pyruvate import is a metabolic vulnerability in androgen receptor-driven prostate cancer. Nat Metab 1(1):70—85.

[23] Olson, K.A., Schell, J.C., Rutter, J., 2016. Pyruvate and metabolic flexibility: illuminating a path toward selective cancer therapies. Trends in biochemical sciences 41(3):219—230.

[24] Beltran, H., Rickman, D.S., Park, K., Chae, S.S., Sboner, A., MacDonald, T.Y., et al., 2011. Molecular characterization of neuroendocrine prostate cancer and identification of new drug targets. Cancer Discov 1(6):487—495.

[25] Alumkal, J.J., Sun, D., Lu, E., Beer, T.M., Thomas, G.V., Latour, E., et al., 2020. Transcriptional profiling identifies an androgen receptor activity-low, stemness program associated with enzalutamide resistance. Proceedings of the National Academy of Sciences of the U S A 117(22):12315—12323.

[26] Brabletz, T., Kalluri, R., Nieto, M.A., Weinberg, R.A., 2018. EMT in cancer. Nature Reviews Cancer 18(2):128—134.

[27] Gorka, J., Marona, P., Kwapisz, O., Waligorska, A., Pospiech, E., Dobrucki, J.W., et al., 2021. MCPIP1 inhibits Wnt/beta-catenin signaling pathway activity and modulates epithelial-mesenchymal transition during clear cell renal cell carcinoma progression by targeting miRNAs. Oncogene 40(50): 6720—6735.

[28] Xiao, Q., Gan, Y., Li, Y., Fan, L., Liu, J., Lu, P., et al., 2021. MEF2A transcriptionally upregulates the expression of ZEB2 and CTNNB1 in colorectal cancer to promote tumor progression. Oncogene 40(19):3364—3377.

[29] Wang, H.J., Pochampalli, M., Wang, L.Y., Zou, J.X., Li, P.S., Hsu, S.C., et al., 2019. KDM8/JMJD5 as a dual coactivator of AR and PKM2 integrates AR/EZH2 network and tumor metabolism in CRPC. Oncogene 38(1):17—32.

[30] Morita, M., Sato, T., Nomura, M., Sakamoto, Y., Inoue, Y., Tanaka, R., et al., 2018. PKM1 confers metabolic advantages and promotes cell-autonomous tumor cell growth. Cancer Cell 33(3):355—367 e357.

[31] Israelsen, W.J., Dayton, T.L., Davidson, S.M., Fiske, B.P., Hosios, A.M., Bellinger, G., et al., 2013. PKM2 isoform-specific deletion reveals a differential requirement for pyruvate kinase in tumor cells. Cell 155(2):397—409.

[32] Dayton, T.L., Gocheva, V., Miller, K.M., Israelsen, W.J., Bhutkar, A., Clish, C.B., et al., 2016. Germline loss of PKM2 promotes metabolic distress and hepatocellular carcinoma. Genes & Development 30(9):1020—1033.

[33] Cookson, M.S., Aus, G., Burnett, A.L., Canby-Hagino, E.D., D'Amico, A.V., Dmochowski, R.R., et al., 2007. Variation in the definition of biochemical recurrence in patients treated for localized prostate cancer: the American Urological Association Prostate Guidelines for Localized Prostate Cancer Update Panel report and recommendations for a standard in the reporting of surgical outcomes. The Journal of Urology 177(2):540—545.

[34] Park, J.W., Lee, J.K., Witte, O.N., Huang, J., 2017. FOXA2 is a sensitive and specific marker for small cell neuroendocrine carcinoma of the prostate. Modern Pathology 30(9):1262—1272.

[35] Tai, S., Sun, Y., Squires, J.M., Zhang, H., Oh, W.K., Liang, C.Z., et al., 2011. PC3 is a cell line characteristic of prostatic small cell carcinoma. The Prostate 71(15):1668—1679.

[36] Chen, W.Y., Wen, Y.C., Lin, S.R., Yeh, H.L., Jiang, K.C., Chen, W.H., et al., 2021. Nerve growth factor interacts with CHRM4 and promotes neuroendocrine differentiation of prostate cancer and castration resistance. Commun Biol 4(1):22.

[37] Xu, H., Chen, J., He, J., Ji, J., Cao, Z., Chen, X., et al., 2021. Serum metabolic profiling identifies a biomarker panel for improvement of prostate cancer diagnosis. Frontiers Oncology 11:666320.